

Toward Directionally Controlled Molecular Motions and Kinetic Intra- and Intermolecular Self-Sorting: Threading Processes of Nonsymmetric Wheel and Axle Components

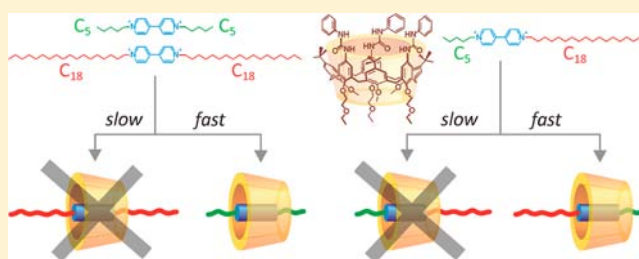
Arturo Arduini,^{*,†} Rocco Bussolati,[†] Alberto Credi,^{*,‡} Andrea Secchi,[†] Serena Silvi,[‡] Monica Semeraro,[‡] and Margherita Venturi^{*,‡}

[†]Dipartimento di Chimica, Università di Parma, Parco Area delle Scienze 17/a, I-43124 Parma, Italy

[‡]Dipartimento di Chimica "G. Ciamician", Università di Bologna, Via Selmi 2, I-40126 Bologna, Italy

S Supporting Information

ABSTRACT: We have investigated the self-assembly of pseudorotaxanes composed of viologen-type axle and calix[6]-arene wheel components. The distinctive feature of this system is that both components are structurally nonsymmetric; hence, their self-assembly can follow four distinct pathways and eventually give rise to two different orientational pseudorotaxane isomers. We found that the alkyl side chains of the viologen recognition site on the molecular axle act as strict kinetic control elements in the self-assembly, thereby dictating which side of the axle pierces the calixarene cavity. Specifically, nonsymmetric axles with alkyl side chains of different length thread the wheel with the shorter chain. Such a selectivity, in combination with the face-selective threading of viologen-type axles afforded by tris(*N*-phenylureido)calix[6]arenes, enables a strict directional control of the self-assembly process for both the face of the wheel and the side of the axle. This kinetic selectivity allows both intramolecular self-sorting between two different side chains in a nonsymmetric axle and intermolecular self-sorting among symmetric axles with alkyl substituents of different length.



INTRODUCTION

Alkyl chains represent the simplest series of substituents in organic compounds. Nevertheless, the conformational space of their molecular backbone determines the possible arrangement and distance of the functional groups attached. This finding has been evidenced by theoretical and experimental studies aimed at quantitatively correlating the properties of compounds that bear *n*-alkyl chains as a function of the chain length.¹ In the case of several polymers, biological membranes, liquid crystals, or functional compounds, the conformational preference of such simple groups has been found to affect substantially the properties and/or reactivity of the other functional groups present in the structure.²

The role played by these structural motif for the construction of supramolecular assemblies or the functioning mode of working devices has usually been considered as an ancillary tool for, e.g., tuning solubility, connecting binding sites, or controlling hydrophobic effects.³ Far less attention has been paid to confer an active role to these groups,⁴ even if literature data indicate that alkyl chains do influence both molecular recognition processes and the switching functionalities of supramolecular assemblies.⁵

An enticing objective is therefore to demonstrate, in a rational manner, that *n*-alkyl chains can be exploited to govern supramolecular assembly/disassembly in time, kinetic control, and space, structural selectivity. Indeed, high-fidelity molecular

recognition is at the basis of the complex functions carried out by biomolecular devices⁶ and is a key requirement⁷ for the development of artificial structures that mimic such features.^{8,9}

Herein we report the results of a structural, thermodynamic and kinetic investigation¹⁰ on the self-assembly of unsophisticated 1,1'-dialkyl-4,4'-bipyridinium (dialkylviologen) guests and a calix[6]arene wheel to afford pseudorotaxanes (see Chart 1).^{11,12} As a working hypothesis, we imagined that the length of the *n*-alkyl side chains attached to the viologen center could guide the ability of these axle-type molecules to enter the cavity of the wheel. To this aim we synthesized (see Scheme 1) a series of symmetric (*Cn**Cn*) and nonsymmetric (*C**S**Cn*) dialkylviologen bis(tosylate) axles and studied their association with wheel **1** by NMR spectroscopy and UV-vis titration and stopped-flow experiments.

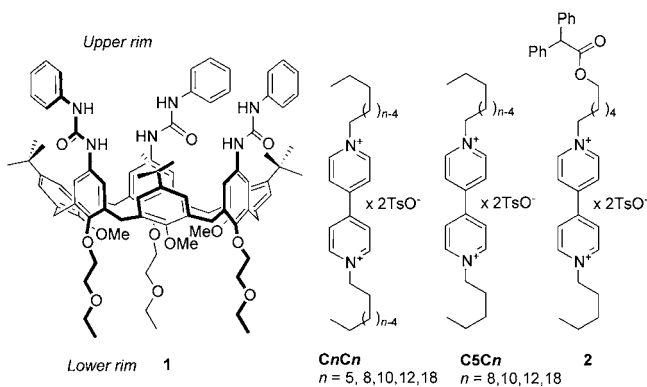
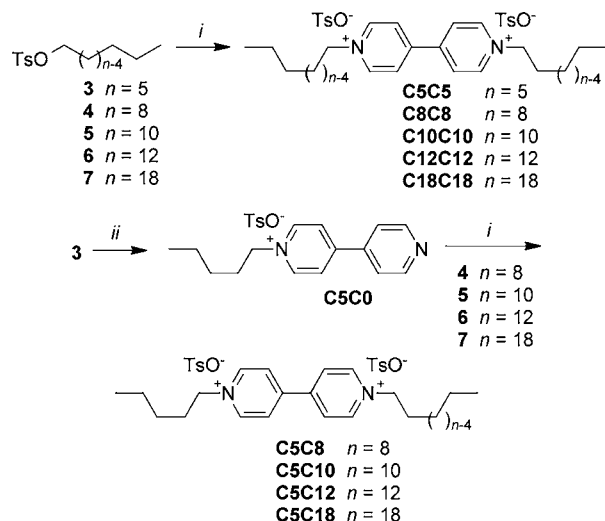
RESULTS AND DISCUSSION

The threading/dethreading of nonsymmetric wheel **1** and nonsymmetric axles *C**S**Cn* is very intriguing under structural and mechanistic viewpoints, because two oriented pseudorotaxane isomers can be obtained by four distinct self-assembly equilibria (see Figure 1). For example, $P[1 \supset C \supset Cn]_{\text{short}}$ may be formed either by piercing **1** from its upper rim with the shorter

Received: April 29, 2013

Published: June 10, 2013

Chart 1. Structure Formulas of the Examined Compounds

Scheme 1^a

^aReagents and conditions: (i) CH₃CN, 100 °C in a glass autoclave, 3 days; (ii) CH₃CN, reflux, 2 days.

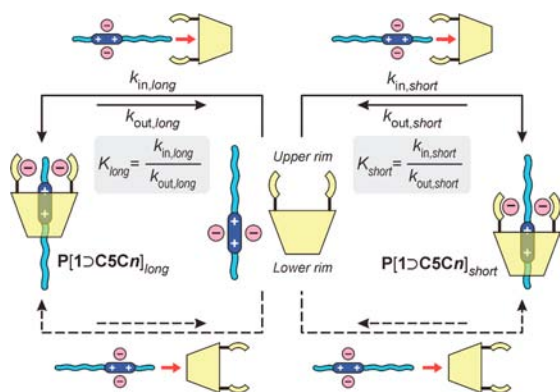


Figure 1. Threading/dethreading equilibria of the two pseudorotaxane isomers P[1⊃C5Cn]_{long} and P[1⊃C5Cn]_{short}. Dashed lines represent lower-rim threading processes that do not occur under our conditions.

alkyl chain of the axle or by passing the longer alkyl chain through the lower rim of the wheel. Previous investigations, however, showed that in apolar solvents threading occurs only through the upper rim, most likely because the ureido groups of **1** bind the counteranions of the axle and favor their dissociation from the viologen dication, which is a prerequisite for the threading process.^{11,12f}

For the same reasons, the viologen unit should pass through the upper rim also on dethreading. Hence, in apolar media, the upper rim of wheel **1** may be threaded by axles C5Cn either through their shorter or longer chains, forming short and long oriented pseudorotaxanes, respectively (top part of Figure 1).^{11b}

To gain insight on these equilibria, in separate experiments a slight excess of solid C5C8, C5C10, C5C12, or C5C18 was added to a solution of wheel **1** in C₆D₆ at 300 K.¹³ The resulting deep-red solution was analyzed by NMR spectroscopy after removal of the excess axle. As observed earlier,¹¹ the ¹H NMR spectra show that in all cases, the calixarene skeleton exhibits a less flexible conformation upon pseudorotaxane formation; indeed, its 12 bridging methylene protons resonate as an AX system. Furthermore, the six ureido NH units of **1** suffer a downfield shift of about 3 ppm, because of their H-bonding with the two tosylate counteranions of the axle. The OMe groups, expelled from the interior of the calixarene cavity upon axle threading, are also downfield shifted and resonate at $\delta = 3.8\text{--}4.1$ ppm (see Figure 2).

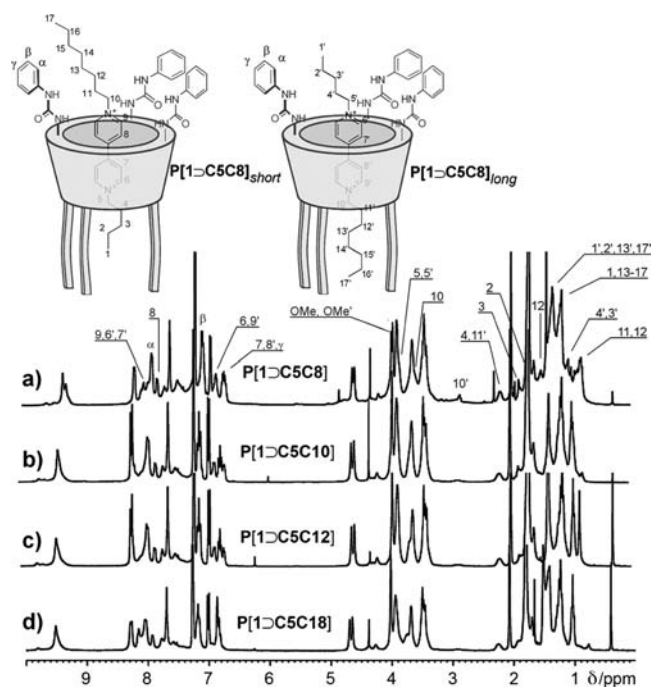


Figure 2. ¹H NMR spectra (300 MHz, C₆D₆, 300 K) of the mixtures of orientational pseudorotaxane isomers obtained by mixing wheel **1** with axles C5Cn-2TsO (n = 8, 10, 12, and 18). The assignment of the axle signals in the case of P[1⊃C5C8] is shown.

When C5C8 was used as the guest, two sets of signals for each of the two alkyl chains linked to the bipyridinium core and two distinct peaks for the methoxy groups of the wheel at ca. 3.9 ppm (see Figure 2a) suggest, in spite of extensive signal overlapping, that the two P[1⊃C5C8]_{short} and P[1⊃C5C8]_{long} isomers are both present in solution. This result indicates that axle C5C8 can thread the upper rim of the wheel with both its alkyl chains, generating the two isomers in a 53:47 ratio, as determined through integration and deconvolution analysis of the two OCH₃ signals of the wheel (see Figure 2a). Similarly, when C5C10 was employed as the guest for **1**, the ¹H NMR (see Figure 2b) and 2D NMR spectra showed the presence of two sets of signals of different magnitude. The more intense

one was attributed to the $P[1\text{C}5\text{C}10]_{\text{short}}$ isomer, whereas the second set with lower intensity was assigned to the $P[1\text{C}5\text{C}10]_{\text{long}}$ isomer, on the basis of some diagnostic signals. Integration and deconvolution analysis of the two OCH_3 peaks indicates that the short and long isomers are formed in a 88:12 ratio.

Different results were obtained when either $\text{C}5\text{C}12$ or $\text{C}5\text{C}18$ were employed as the axles. Only one set of signals was observed in the ^1H NMR analyses (see Figure 2c,d), and 2D ROESY experiments (see Figure 3 and SI) evidenced that the

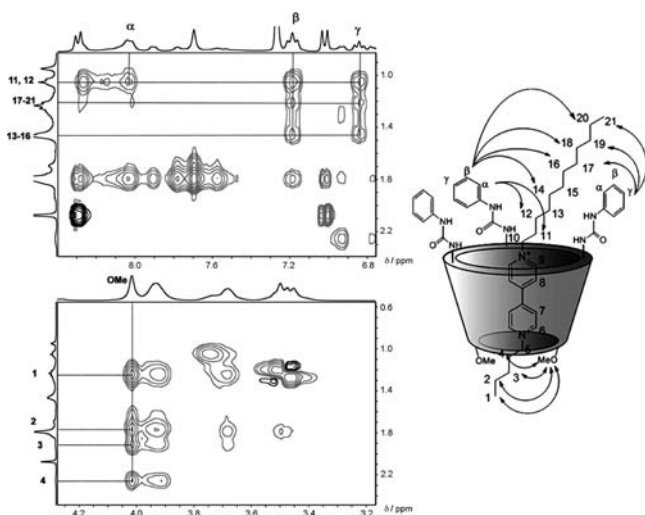


Figure 3. Expanded regions of the ROESY spectra (300 MHz, C_6D_6 , spinlock = 200 ms) of the pseudorotaxane $P[1\text{C}5\text{C}12]_{\text{short}}$.

pentyl chain of the axle is in proximity of the lower rim of the wheel. These findings clearly indicate that $\text{C}5\text{C}12$ and $\text{C}5\text{C}18$ thread the wheel through their shorter alkyl chain, affording exclusively the $P[1\text{C}5\text{C}12]_{\text{short}}$ and $P[1\text{C}5\text{C}18]_{\text{short}}$ isomers.

To establish whether, for each axle, the orientational outcome is dictated by kinetic reasons or by a different thermodynamic stability of the two isomers, all the mixtures described above were refluxed for 24 h and then subjected to NMR analysis (see Figure 4). With the only exception of $P[1\text{C}5\text{C}18]$, the spectra exhibited two resonances for the methoxy groups of the wheel. Deconvolution of these signals show that the $P[1\text{C}5\text{C}n]_{\text{short}}$ and $P[1\text{C}5\text{C}n]_{\text{long}}$ species ($n = 10$ and 12) are in a 1:1 ratio (see Figure 4b,c); thus, heating promoted the isomerization of the short pseudorotaxane isomer to the corresponding long one. These results suggest that, under the employed conditions, the two pseudorotaxane isomers have comparable thermodynamic stability. The conversion of $P[1\text{C}5\text{C}18]_{\text{short}}$ to $P[1\text{C}5\text{C}18]_{\text{long}}$ was only 20% after the same heating period (See Figure 4d) and 30% upon refluxing for 10 days. These data enable us to conclude that in C_6D_6 dethreading is much slower than threading and that a very strict kinetic control of the product is achieved, particularly in the case of the $\text{C}5\text{C}12$ and $\text{C}5\text{C}18$ axles. Such a slow dethreading, which determines the incomplete isomerization of $P[1\text{C}5\text{C}18]$, can be ascribed to the increased insolubility of the nonsymmetric axles with longer alkyl chains in C_6D_6 , most likely accompanied by formation of aggregates.¹⁴ The strong solvophobic effects that stabilize the axle–wheel complex are also responsible for the large kinetic barrier for the dethreading.

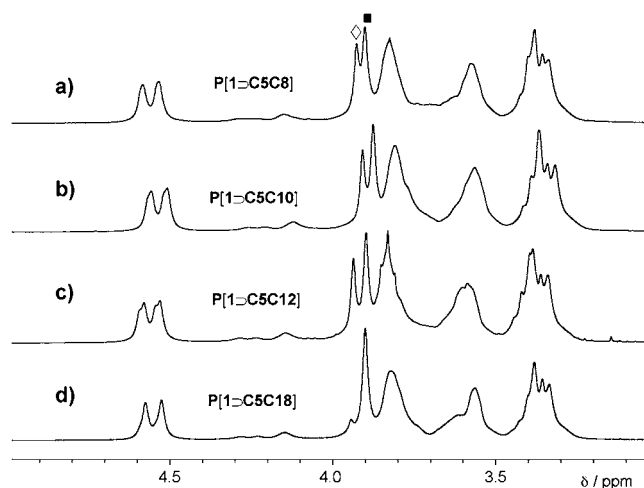


Figure 4. Expanded ^1H NMR spectra (300 MHz, C_6D_6 , 300 K) of the $P[1\text{C}5\text{C}8]$ (a), $P[1\text{C}5\text{C}10]$ (b), $P[1\text{C}5\text{C}12]$ (c), and $P[1\text{C}5\text{C}18]$ (d) pseudorotaxanes after refluxing in C_6D_6 for 24 h. The signal of the methoxy groups in the short and long orientational isomers is marked with symbol (■) and (◇), respectively.

To disclose whether this chain-length selectivity of the wheel toward $\text{C}5\text{C}n$ axles could be exploited for the sorting of two different guests, competitive experiments were carried out. To a C_6D_6 solution of **1** an excess of a 1:1 solid mixture of $\text{C}5\text{C}5$ and $\text{C}18\text{C}18$ was added at room temperature. After 1 h of stirring, the excess undissolved salts were removed by filtration, and the solution submitted to ^1H NMR analysis. Even though NMR techniques do not allow the detection of trace amounts, the ^1H NMR spectrum strongly suggests the presence of $P[1\text{C}5\text{C}5]$ as the unique pseudorotaxane specie present in solution. No signals assignable to the $P[1\text{C}18\text{C}18]$ complex could be indeed detected. The NMR sample was then diluted with methanol and submitted to ESI-MS analysis that unequivocally confirmed the absence of both the pseudorotaxane $P[1\text{C}18\text{C}18]$ and the free axle $\text{C}18\text{C}18$ (see SI).

In order to further support this conclusion and extend it to the conditions employed in the UV–vis experiments (vide infra), we studied the formation of the pseudorotaxanes in homogeneous solutions of dichloromethane, a solvent in which the free axles are also soluble. Indeed, by mixing the axle and wheel components (ca. 10^{-4} M) in CD_2Cl_2 at 300 K, a 1:1 mixture of both oriented pseudorotaxane isomers was obtained (within the time needed for sample preparation and data acquisition) for all the $\text{C}5\text{C}n$ axles.

Although we showed earlier that in apolar media threading of viologen axles through the lower rim of **1** does not occur,^{11,12f} we devised an experiment to probe whether the rearrangement of the $P[1\text{C}5\text{C}n]_{\text{short}}$ isomer to $P[1\text{C}5\text{C}n]_{\text{long}}$ can take place via lower-rim threading of the latter. To this aim, CD_2Cl_2 solutions of wheel **1** and stoppered axle **2**^{11a} (see Chart 1) were mixed, and the NMR spectrum was monitored over 4 days. The data collected unambiguously showed that only the pseudorotaxane with the diphenylacetyl stopper located at the upper rim of the wheel was formed, thus confirming that lower-rim threading does not occur.

The thermodynamic and kinetic aspects of the assembly of the $P[1\text{C}5\text{C}n]$ pseudorotaxanes in CH_2Cl_2 were also thoroughly investigated by means of steady-state (spectrophotometric titrations) and time-resolved (stopped-flow experiments) UV–vis spectra. The addition of **1** to a solution of the

C5C*n* axles causes changes in the UV absorption bands of the molecular components and the appearance of a characteristic charge transfer band at around 460 nm (see, e.g., Figure 5).^{11c,12f,15} The least-squares nonlinear fitting of the absorption

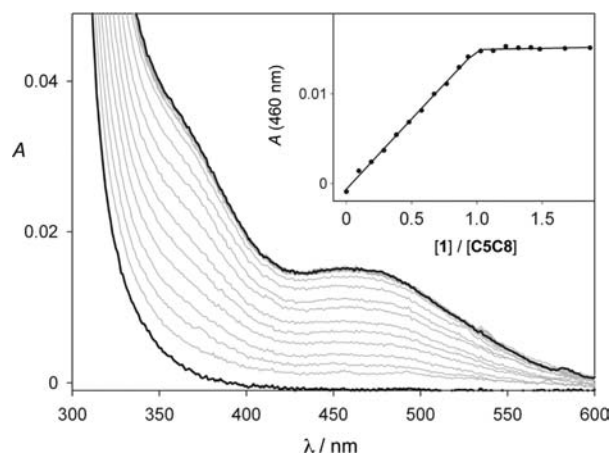


Figure 5. Absorption spectra of a 2.9×10^{-5} M solution of C5C8 in CH_2Cl_2 upon addition of 1. The inset shows the absorption changes at 460 nm together with the fitted curve corresponding to a 1:1 binding model.

data collected in each titration experiment with a 1:1 binding model yielded association constants that refer to the simultaneous formation of the two pseudorotaxane isomers $\text{P}[\text{1}\text{D}\text{C5Cn}]_{\text{short}}$ and $\text{P}[\text{1}\text{D}\text{C5Cn}]_{\text{long}}$. As the NMR analysis shows that these two species have the same stability, the association constant of the individual isomers can be determined (SI). The values are listed in Table 1, together with those of the association constants measured for the symmetric C*n*C*n* and the stoppered 2 axles.

Table 1. Thermodynamic and Kinetic Data for the Association of Axles C5C*n*, C*n*C*n*, and 2 with wheel 1 (CH_2Cl_2 , 293 K)

entry	axle	$\log K^a$	$k_{\text{in}} (\text{M}^{-1} \text{s}^{-1})^b$	$k_{\text{out}} (\text{s}^{-1})^c$
1	C5C5	6.7 ± 0.3	$(2 \pm 1) \times 10^8$	40
2	C8C8	6.7 ± 0.4	$(2 \pm 1) \times 10^6$	0.4
3	C12C12	5.6 ± 0.2	260 ± 30	7×10^{-4}
4	C18C18	5.1 ± 0.2	150 ± 20	1×10^{-3}
5	2 ^d	6.5 ± 0.2	$(5.8 \pm 0.1) \times 10^7$	19
6	C5C8	>7	$(2 \pm 1) \times 10^8$	<20
7	C5C12	>7	$(2 \pm 1) \times 10^8$	<20
8	C5C18	>7	$(2 \pm 1) \times 10^8$	<20

^aDetermined by spectrophotometric titrations. The value reported for the nonsymmetric axles refers to the individual short and long pseudorotaxane isomers; $K = K_{\text{short}} = K_{\text{long}}$. ^bDetermined by stopped-flow experiments. ^c $k_{\text{out}} = k_{\text{in}}/K$. ^dFrom ref 14.

The association constants for the C5C8, C5C12 and C5C18 nonsymmetric axles are very large, irrespective of the length of the longer alkyl chain. Furthermore, the values correspond, within the experimental error, to the association constants determined for the C5C5 and C8C8 symmetric axles and the stoppered axle 2, which in turn are comparable with those previously measured on similar systems.^{11c,12f,15} Conversely, the association constants obtained for axles C12C12 and C18C18 are more than 1 order of magnitude smaller; this is a somewhat

surprising result, considering that the length of the alkyl chain has no effect on the stability of the pseudorotaxanes comprising nonsymmetric axles (vide supra). We ascribe this behavior to the fact that the free axles bearing long alkyl chains are stabilized by the formation of aggregates in apolar solvents, even in dilute solutions.¹⁴

The threading rate constants (k_{in}) for pseudorotaxane assembly were measured by performing stopped-flow experiments, in which the absorption increase at 258 nm observed upon mixing wheel and axle was monitored over time (See Figure 6 and SI). The data were fitted with a mixed order model $A + B \rightleftharpoons C$, by fixing the equilibrium constants to the values determined in the titration experiments (Table 1).

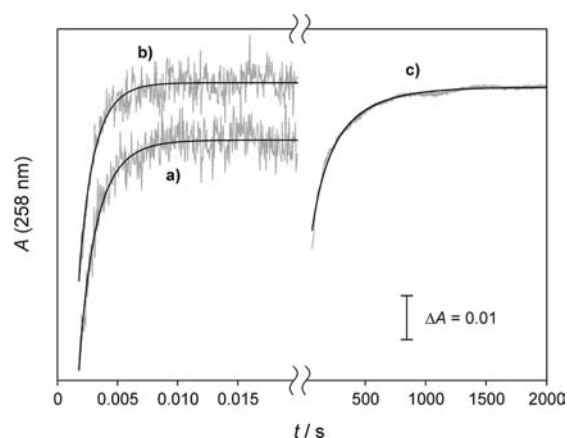


Figure 6. Time-dependent absorption changes at 258 nm recorded upon mixing 1 and either (a) C5C18, (b) C5C5, or (c) C18C18 in CH_2Cl_2 at 293 K. The solid lines represent the data fitting. Note the different time scale for (a) and (b) with respect to (c). Concentration of the compounds after mixing, 8×10^{-6} M axle and 1.0×10^{-5} M wheel (a and b), 1.2×10^{-5} M axle and 2.0×10^{-5} M wheel (c); optical path length, 1.00 cm; final absorbance values, 0.91 (a and b) and 1.39 (c).

The C*n*C*n* symmetric axles show threading rate constants that depend strongly on the alkyl chain length; as expected, the threading is slower for axles with longer chains (entries 1–4 in Table 1). Specifically, C12C12 and C18C18 exhibit a similar k_{in} value, which is 4 and 6 orders of magnitude lower than the values determined for C8C8 and C5C5, respectively. This effect can be rationalized considering that the degrees of freedom of the alkyl chain, and thus the entropic price for threading, increase by increasing its length. The data obtained for the C5C*n* nonsymmetric axles (entries 6–8 in Table 1) show that they thread the wheel with the same rate constant, which agrees with k_{in} found for C5C5 (entry 1) and 2 (entry 5). These results clearly point to a common threading mode, involving the slipping of the shorter chain of the nonsymmetric axles through the upper rim of the wheel; in other words, the observed k_{in} (Table 1) corresponds precisely to $k_{\text{in,short}}$ in Figure 1.

The dethreading rate constants, k_{out} , have been estimated from the kinetic and thermodynamic data (Table 1); in the case of the $\text{P}[\text{1}\text{D}\text{C5Cn}]$ pseudorotaxanes they correspond to $k_{\text{out,short}}$ in Figure 1. The obtained k_{out} values evidence, in line with expectations, that dethreading as well as threading occurs from the upper rim. This dethreading mode is indeed clearly supported by the following data: (i) the k_{out} of the nonsymmetric axles is equal to that found for axle 2 which, because of the presence of the stopper, dethreads exclusively

from the upper rim of the wheel; and (ii) if dethreading would occur from the lower rim (for both the symmetric and nonsymmetric axles), the k_{out} estimated for C5C8, C5C12, and C5C18 should be similar to the k_{out} of the corresponding symmetric axles C8C8, C12C12 and C18C18.

The values of the dethreading rate constants also show that the axle cannot come out of the wheel within the threading time period (see Figure 6a). P[1D5C5Cn]_{short} however, can dethread within seconds, and P[1D5C5Cn]_{long} may be formed in a few minutes under our conditions (see, e.g., k_{in} for C18C18 and Figure 6c), in full agreement with the pseudorotaxane isomerization observed from NMR spectra in dilute CD₂Cl₂. Unfortunately, such a process cannot be seen in the stopped-flow experiments because the short and long species have identical spectra, and hence there is no signal to monitor.

CONCLUSION

In conclusion, we have shown that simple *n*-alkyl side chains in viologen-type molecular axles act as kinetic control elements in the self-assembly of calix[6]arene pseudorotaxanes. The investigated system displays both intra- and intermolecular self-sorting capabilities, by virtue of the kinetic selectivity toward alkyl chains of different lengths. When nonsymmetric axles are mixed with the (inherently nonsymmetric) calixarene wheel under appropriate conditions, only one out of two equally stable oriented pseudorotaxane isomers is obtained. Such a strict kinetic control guides the self-assembly process through one of four possible threading/dethreading mechanisms (see Figure 1). To our knowledge, this is the first case of host-guest self-assembly that exhibits selectivity for both the host face^{11,12} and the guest side. On the other hand, when symmetric axles are mixed with the calixarene, the wheel can sort the guest with the shortest chains, and only one pseudorotaxane is formed. These results are relevant for the development of supramolecular systems endowed with sophisticated functionalities, such as directionally controlled molecular motions⁷ and kinetic self-sorting.^{7a,c,9e-g,16} Computational and experimental studies aimed at gaining a deeper understanding on these processes and exploiting them to make functional devices are underway in our laboratories.

EXPERIMENTAL SECTION

General. All the reagents were of reagent grade quality obtained from commercial suppliers and were used without further purification. Melting points are uncorrected. NMR spectra were recorded using the residual solvent signals as an internal reference. Mass analyses were carried out in the ESI mode. Calix[6]arene "wheel" **1** and stoppered axle **2**,^{11a} compounds **3**,¹⁷ **4**,¹⁸ **5**,¹⁹ **6**,²⁰ **7**,²¹ C5C0,²¹ and C8C8²² were synthesized according to literature procedures. Deuterated benzene was used as the solvent in most NMR experiments because a better resolution of the signals, especially in the low fields portion of the spectra, is afforded. The use of deuterated dichloromethane for NMR structural determinations, because of extensive signal overlapping, can be hardly employed to analyze a single orientational isomer and is useless for a mixture of the two isomers. On the other hand, benzene could not be employed for UV-vis titration and kinetic experiments because the free axles are insoluble in this solvent.

Absorption spectra were recorded with a Perkin-Elmer Lambda45 and Lambda650 spectrophotometers, on air equilibrated CH₂Cl₂ (Merck Uvasol) solutions at room temperature (ca. 298 K), with concentrations ranging from 1×10^{-5} to 2×10^{-4} M. Solutions were examined in 1 cm spectrofluorimetric quartz cells. The experimental error on the wavelength values was estimated to be ± 1 nm. Reaction kinetic profiles were collected on air-equilibrated CH₂Cl₂ (Romil) solutions at 298 K with an Applied Photophysics SX 18-MV

equipment. The standard flow tube used had an observation path length of 1.0 cm, and the driving ram for the mixing system was operated at the recommended pressure of 8.5 bar. Under these conditions the time required to fill the cell was 1.35 ms (based on a test reaction). A baseline correction was applied to the stopped-flow traces, to take into account the dependence of the instrument response on pressure. In all the experiments, the cell block and drive syringes were thermostatted by using a circulating constant-temperature bath maintained at the required temperature. In all cases the data were elaborated by means of the SPECFIT fitting program.²³

General Procedure for the Synthesis of Compounds C5Cn. A solution of compound C5C0 (0.4 g, 1.0 mmol) and the appropriate tosylate derivative 4–7 (1.5 mmol) in CH₃CN (50 mL) was poured in a 100 mL glass autoclave flask. After few vacuum–nitrogen cycles, the glass autoclave was sealed, and the reaction mixture was refluxed for 3 days. After cooling to room temperature, the solvent was evaporated under reduced pressure, and the residue was taken up with few portions of hot ethyl acetate (3 \times 20 mL) until the desired viologen salts precipitated from the trituration solvent as a solid compound. The solid was recovered by suction filtration and purified by recrystallization from CH₃CN to afford product C5Cn as a white solid.

C5C8. (0.5 g, 75% yield), ¹H NMR (300 MHz, CD₃OD): δ = 9.26 (d, *J* = 6.0, 4H), 8.67 (d, *J* = 6.0, 4H), 7.70 (d, *J* = 7.8, 4H), 7.24 (d, *J* = 7.8, 4H), 4.74 (t, *J* = 7.5, 4H), 2.38 (s, 6H), 2.2–2.0 (m, 4H), 1.5–1.3 (m, 14H), 1.1–0.9 (m, 6H); ¹³C NMR (100 MHz, CD₃OD): δ = 149.8, 145.7, 142.3, 140.3, 128.5, 126.9, 125.5, 61.9, 31.5, 31.2, 30.8, 28.8, 28.7, 27.9, 25.8, 22.3, 21.8, 19.9, 13.0, 12.7; MS (ES): *m/z* (%): 511 (30) [M – TsO]⁺, 339 (60) [M – 2TsO – H]⁺; mp = 197.5–199.8 °C.

C5C10. (0.5 g, 75% yield), ¹H NMR (300 MHz, CD₃OD): δ = 9.24 (d, *J* = 6.9, 4H), 8.65 (d, *J* = 6.9, 4H), 7.69 (d, *J* = 8.1, 4H), 7.24 (d, *J* = 8.1, 4H), 4.73 (t, *J* = 7.5, 4H), 2.38 (s, 6H), 2.2–2.0 (m, 4H), 1.5–1.3 (m, 18H), 1.1–0.9 (m, 6H); ¹³C NMR (100 MHz, CD₃OD): δ = 149.8, 145.6, 142.3, 140.3, 128.5, 126.9, 125.5, 61.9, 31.6, 31.1, 30.8, 29.2, 29.0, 28.7, 27.9, 25.8, 22.3, 21.8, 19.9, 13.0, 12.7; MS (ES): *m/z* (%): 367 [M – 2TsO – H]⁺; mp = 188.5–191.8 °C.

C5C12. (0.5 g, 70% yield), ¹H NMR (300 MHz, CD₃OD): δ = 9.25 (d, *J* = 6.9, 4H), 8.66 (d, *J* = 6.9, 4H), 7.69 (d, *J* = 8.1, 4H), 7.24 (d, *J* = 8.1, 4H), 4.73 (t, *J* = 7.5, 4H), 2.38 (s, 6H), 2.2–2.0 (m, 4H), 1.5–1.3 (m, 22H), 1.1–0.9 (m, 6H); ¹³C NMR (100 MHz, CD₃OD): δ = 149.8, 145.6, 142.3, 140.3, 128.5, 126.9, 125.5, 61.9, 31.7, 31.2, 30.8, 29.3, 29.2, 29.1, 29.0, 28.8, 27.9, 25.8, 22.32, 21.8, 19.9, 13.0, 12.7; MS (ES): *m/z* (%): 567 [M – TsO]⁺, 395 [[M – 2TsO – H]⁺]; mp = 167.2–172.3 °C.

C5C18. (0.65 g, 80% yield), ¹H NMR (300 MHz, CD₃OD): δ = 9.26 (d, *J* = 6.6, 4H), 8.66 (d, *J* = 6.6, 4H), 7.69 (d, *J* = 8.1, 4H), 7.24 (d, *J* = 8.1, 4H), 4.73 (t, *J* = 7.5, 4H), 2.38 (s, 6H), 2.2–2.0 (m, 4H), 1.5–1.3 (m, 34H), 1.1–0.9 (m, 6H); ¹³C NMR (100 MHz, CD₃OD): δ = 149.8, 145.7, 140.3, 128.5, 126.8, 125.5, 61.9, 31.7, 31.2, 30.8, 29.4, 29.3, 29.1, 29.0, 28.8, 27.9, 25.9, 22.34, 21.79, 19.9, 13.1, 12.8; MS (ES): *m/z* (%): 395 [[M – 2TsO – H]⁺]; mp = 169.1–172.3 °C.

General Procedure for the Synthesis of Compounds CnCn. The procedure is identical to that described for the synthesis of C5Cn using, however, 4,4'-bipyridine (0.4 g, 2.5 mmol) and tosylates 3–7 (3.5 mmol) as starting materials.

C5C5. (0.5 g, 80% yield), ¹H NMR (300 MHz, CD₃OD): δ = 9.24 (d, *J* = 6.6, 4H), 8.65 (d, *J* = 6.6, 4H), 7.69 (d, *J* = 8.4, 4H), 7.23 (d, *J* = 8.4, 4H), 4.72 (t, *J* = 7.5, 4H), 2.37 (s, 6H), 2.1–2.0 (m, 4H), 1.5–1.3 (m, 8H), 0.92 (t, *J* = 7.2, 6H); ¹³C NMR (100 MHz, CD₃OD): δ = 149.8, 145.6, 142.3, 140.3, 128.5, 126.9, 61.9, 30.8, 27.9, 21.8, 19.9, 12.7; MS (ES): *m/z* (%): 663 [M + Na]⁺, 297 [M – 2TsO – H]⁺; mp = 215.5–216.8 °C.

C10C10. (0.6 g, 70% yield), ¹H NMR (300 MHz, CD₃OD): δ = 9.26 (d, *J* = 6.6, 4H), 8.66 (d, *J* = 6.6, 4H), 7.70 (d, *J* = 8.4, 4H), 7.24 (d, *J* = 8.4, 4H), 4.74 (t, *J* = 7.5, 4H), 2.39 (s, 6H), 2.1–2.0 (m, 4H), 1.5–1.3 (m, 20H), 0.92 (t, *J* = 7.2, 6H); ¹³C NMR (100 MHz, CD₃OD): δ = 148.3, 144.5, 140.7, 138.8, 126.9, 125.3, 124.0, 61.8, 30.1, 29.6, 27.7, 27.6, 27.5, 27.2, 24.3, 20.7, 18.4, 11.5; MS (ES): *m/z* (%): 440 [M – 2TsO + H]²⁺; mp = 195.5–196.8 °C.

C12C12. (0.7 g, 80% yield), ^1H NMR (300 MHz, CD_3OD): $\delta = 9.24$ (d, $J = 6.6$, 4H), 8.65 (d, $J = 6.6$, 4H), 7.69 (d, $J = 8.1$, 4H), 7.23 (d, $J = 8.1$, 4H), 4.73 (t, $J = 7.5$, 4H), 2.38 (s, 6H), 2.1–2.0 (m, 4H), 1.5–1.3 (m, 36H), 0.92 (t, $J = 7.2$, 6H); ^{13}C NMR (100 MHz, CD_3OD): $\delta = 149.8$, 145.6, 140.3, 128.5, 126.9, 125.5, 61.9, 31.6, 31.1, 29.3, 29.2, 29.1, 29.0, 28.8, 25.8, 22.3 19.9, 13.0; MS (ES): m/z (%): 247 $[\text{M} - 2\text{TsO}]^+$; mp = 183.5–184.5 °C.

C18C18. (0.5 g, 50% yield), ^1H NMR (300 MHz, CD_3OD): $\delta = 9.25$ (d, $J = 6.7$, 4H), 8.65 (d, $J = 6.7$, 4H), 7.68 (d, $J = 8.1$, 4H), 7.22 (d, $J = 8.1$, 4H), 4.72 (t, $J = 7.6$, 4H), 2.36 (s, 6H), 2.1–2.0 (m, 4H), 1.5–1.3 (m, 60H), 0.89 (t, $J = 6.9$, 6H); ^{13}C NMR (100 MHz, CD_3OD): $\delta = 149.8$, 145.6, 140.2, 128.4, 126.8, 125.5, 61.8, 31.6, 31.6, 31.1, 29.3, 29.2, 29.1, 29.0, 28.7, 25.8, 22.3 19.9, 13.0; MS (ES): m/z (%): 834 $[\text{M} - \text{TsO}]^+$; mp = 172.5–174.5 °C.

General Procedure for the Preparation of the Pseudorotaxane Complexes. Calix[6]arene wheel **1** (10 mg, 0.007 mmol) and a slight excess of the appropriate axle (**C5C8**–**C5C18**) (0.01 mmol) were equilibrated in 0.5 mL of C_6D_6 at 300 K for 1 h, until the solution turns to a deep-red color. The excess of axle was removed by filtration, and the homogeneous solution obtained was characterized through NMR techniques.

P[1C5C8]. ^1H NMR (300 MHz, C_6D_6): $\delta = 9.35$ (m, 6H), 8.15 (d, $J = 6.2$, 4H), 8.00–8.10 (m, 2H), 7.87 (bs, 6H), 7.78 (bs, 2H), 7.66 (bs, 3H), 7.57 (s, 6H), 7.44 (bs, 3H), 6.9–7.1 (m, 6H), 6.90 (d, $J = 6.2$, 4H), 6.70 (bs, 2H), 6.6–6.7 (m, 5H), 4.55 (d, $J = 14.2$, 6H), 3.93–3.90 (s, 9H), 3.84 (bs, 8H), 3.58 (bs, 8H), 3.3–3.4 (m, 12H), 2.80 (bs, 2H), 2.24 (bs, 2H), 1.96 (s, 6H), 1.67 (bs, 2H), 1.58 (s, 29H), 1.28 (bs, 2H), 1.0–1.2 (m, 25H), 0.7–0.9 (m, 8H).

P[1C5C10]. ^1H NMR (300 MHz, C_6D_6): $\delta = 9.36$ (m, 6H), 8.0–8.2 (m, 6H), 7.90 (bs, 6H), 7.75 (bs, 2H), 7.65 (bs, 3H), 7.55 (s, 6H), 7.43 (bs, 3H), 7.05 (t, $J = 7.5$, 6H), 6.88 (d, $J = 6.5$, 4H), 6.79 (d, $J = 5.4$, 2H), 6.69 (t, $J = 7.5$, 3H), 6.64 (d, $J = 5.4$, 2H), 4.52 (d, $J = 15.0$, 6H), 3.88 (s, 9H), 3.80 (bs, 8H), 3.56 (bs, 8H), 3.3–3.4 (m, 12H), 2.12 (bs, 2H), 1.94 (s, 6H), 1.80 (bs, 2H), 1.65 (s, 29H), 1.30 (bs, 16H), 1.0–1.2 (m, 19H), 0.7–0.9 (m, 4H).

P[1C5C12]. ^1H NMR (300 MHz, C_6D_6): $\delta = 9.52$ (m, 6H), 8.2–8.3 (m, 6H), 8.05 (bs, 6H), 7.90 (bs, 2H), 7.78 (bs, 3H), 7.70 (s, 6H), 7.57 (bs, 3H), 7.20 (t, $J = 7.5$, 6H), 7.02 (d, $J = 6.5$, 4H), 6.93 (d, $J = 5.3$, 2H), 6.85 (t, $J = 7.5$, 3H), 6.78 (d, $J = 5.3$, 2H), 4.55 (d, $J = 15.0$, 6H), 3.93 (s, 9H), 3.85 (bs, 8H), 3.65 (bs, 8H), 3.3–3.5 (m, 12H), 2.26 (bs, 2H), 2.07 (s, 6H), 1.90 (bs, 2H), 1.80 (s, 29H), 1.45 (bs, 16H), 1.1–1.3 (m, 23H), 1.05 (bs, 4H).

P[1C5C18]. ^1H NMR (300 MHz, C_6D_6): $\delta = 9.52$ (m, 6H), 8.29 (bs, 4H), 8.15 (bs, 2H), 8.05 (bs, 6H), 7.93 (bs, 2H), 7.79 (bs, 3H), 7.70 (s, 6H), 7.60 (bs, 3H), 7.20 (bs, 6H), 7.03 (d, $J = 6.5$, 4H), 6.8–6.9 (m, 7H), 4.66 (d, $J = 15.0$, 6H), 3.93 (s, 9H), 3.85 (bs, 8H), 3.65 (bs, 8H), 3.3–3.5 (m, 12H), 2.26 (bs, 2H), 2.07 (s, 6H), 1.90 (bs, 2H), 1.80 (s, 29H), 1.45 (bs, 28H), 1.1–1.3 (m, 23H), 1.05 (bs, 4H).

Determination of the Stability Constants of Orientational Isomers from Spectroscopic Titrations. The reactions corresponding to the formation of the short and long orientational isomers are

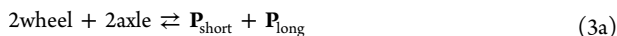


$$K_{\text{short}} = [\text{P}_{\text{short}}]/[\text{wheel}][\text{axle}] \quad (1b)$$



$$K_{\text{long}} = [\text{P}_{\text{long}}]/[\text{wheel}][\text{axle}] \quad (2b)$$

The overall self-assembly process can be represented by the sum reaction:



$$K_{\text{sum}} = [\text{P}_{\text{short}}][\text{P}_{\text{long}}]/[\text{wheel}]^2[\text{axle}]^2 = K_{\text{short}} \times K_{\text{long}} \quad (3b)$$

The short and long pseudorotaxane isomers, however, have identical UV–vis absorption spectra and cannot be distinguished in spectrophotometric titrations. Hence, reaction 3a becomes 4a, which in turn can be reduced to a 1:1 equilibrium 5a that describes the experimentally observed behavior:



$$K_{\text{sum}} = [\text{P}]^2/[\text{wheel}]^2[\text{axle}]^2 \quad (4b)$$



$$K_{1:1} = (K_{\text{sum}})^{1/2} \quad (5b)$$

NMR Experiments demonstrated that the two orientational isomers are equally stable in CH_2Cl_2 , i.e., $K_{\text{short}} = K_{\text{long}}$. Thus, according to eqs 3b and 5b, $K_{\text{short}} = K_{\text{long}} = (K_{\text{sum}})^{1/2} = K_{1:1}$. In conclusion, the system can be described with a 1:1 binding model, and the association constant obtained from the fitting of the titration curve corresponds to the stability constant of each individual isomer. In all cases the data were elaborated by means of the SPECFIT fitting program.²³

■ ASSOCIATED CONTENT

Supporting Information

1D and 2D NMR spectra in C_6D_6 of the pseudorotaxanes series **P[1C5C*n*]**, UV–vis absorption spectrum of a mixture of **1** and **C12C12** in CH_2Cl_2 , and time-dependent absorption changes (kinetic experiments) recorded for pseudorotaxane complexes **P[1C5C8]**, **P[1C5C12]**, **P[1C5C8C8]**, and **P[1C5C12C12]** in CH_2Cl_2 at 293 K. This material is available free of charge via the Internet at <http://pubs.acs.org>.

■ AUTHOR INFORMATION

Corresponding Author

arturo.arduini@unipr.it; alberto.credi@unibo.it; margherita.venturi@unibo.it

Notes

The authors declare no competing financial interest.

■ ACKNOWLEDGMENTS

This work was supported by the Italian MIUR (PRIN 2010CX2TLM) and the Universities of Bologna and Parma. We thank CIM (Centro Interdipartimentale di Misura) “G. Casnati” of the University of Parma for NMR and MS measurements.

■ REFERENCES

- (a) Smith, B.; Siepmann, J. I. *Science* **1994**, *264*, 1118. (b) Berardi, R.; Spinozzi, F.; Zannoni, C. *Chem. Phys. Lett.* **1996**, *260*, 633. (c) Göttlich, R.; Kahrs, B. C.; Krüger, J.; Hoffmann, R. W. *Chem. Commun.* **1997**, *3*, 247. (d) Bhattacharyya, S. N.; Patterson, D. J. *Phys. Chem.* **1979**, *83*, 2979. (e) Bessières, D.; Piñeiro, M. M.; De Ferron, G.; Plantier, F. J. *Chem. Phys.* **2010**, *133*, 074507.
- (a) Goodsaid-Zalduondo, F.; Engelman, D. M. *Biophys. J.* **1981**, *35*, 587. (b) Nakaoki, T.; Nagano, H.; Yanagida, T. *J. Mol. Struct.* **2004**, *699*, 1.
- (3) See, e.g.: (a) Smithrud, D. B.; Sanford, E. M.; Chao, I.; Ferguson, S. B.; Carcanague, D. R.; Evanseck, J. D.; Houk, V.; Diederich, F. *Pure Appl. Chem.* **1990**, *62*, 2227. (b) *Comprehensive Supramolecular Chemistry*; Szejtli, J.; Osa, T., Eds.; Pergamon Press: Oxford, 1996; Vol. 3. (c) Nepogodiev, S. A.; Stoddart, J. F. *Chem. Rev.* **1998**, *98*, 1959.
- (4) Jiang, W.; Ajami, D.; Rebek, Jr., J. J. *Am. Chem. Soc.* **2012**, *134*, 8070.
- (5) See, e.g.: (a) Clifford, T.; Abushamleh, A.; Busch, D. H. *Proc. Natl. Acad. Sci. U.S.A.* **2002**, *99*, 4830. (b) Venturi, M.; Dumas, S.; Balzani, V.; Cao, J.; Stoddart, J. F. *New J. Chem.* **2004**, *28*, 1032. (c) Arduini, A.; Bussolati, R.; Credi, A.; Pochini, A.; Secchi, A.; Silvi, S.; Venturi, M. *Tetrahedron* **2008**, *64*, 8279. (d) Gattuso, G.; Notti, A.; Parisi, M. F.; Pisagatti, I.; Amato, M. E.; Pappalardo, A.; Pappalardo, S. *Chem.—Eur. J.* **2010**, *16*, 2381. (e) Arduini, A.; Bussolati, R.; Masseroni, D.; Royal, G.; Secchi, A. *Eur. J. Org. Chem.* **2012**, 1033.
- (6) (a) *Molecular Motors*; Schliwa, M., Ed.; Wiley-VCH: Weinheim, 2002; (b) Goodsell, D. S. *Bionanotechnology – Lessons from Nature*;

Wiley: Hoboken, 2004; (c) Mann, S. *Angew. Chem., Int. Ed.* **2008**, *47*, 2.

(7) (a) Safont-Sempere, M. M.; Fernández, G.; Würthner, F. *Chem. Rev.* **2011**, *111*, 5784. (b) Coskun, A.; Banaszak, M.; Astumian, R. D.; Stoddart, J. F.; Grzybowski, B. A. *Chem. Soc. Rev.* **2012**, *41*, 19. (c) Saha, M. L.; Schmittel, M. *Org. Biomol. Chem.* **2012**, *10*, 4651.

(8) (a) Kinbara, K.; Aida, T. *Chem. Rev.* **2005**, *105*, 1377. (b) Browne, W. R.; Feringa, B. L. *Nat. Nanotechnol.* **2006**, *1*, 25. (c) Ma, X.; Tian, H. *Chem. Soc. Rev.* **2010**, *39*, 70. (d) Silvi, S.; Venturi, M.; Credi, A. *Chem. Commun.* **2011**, *47*, 2483.

(9) Recent examples: (a) Wang, J.; Feringa, B. L. *Science* **2011**, *331*, 1429. (b) Haberhauer, G. *Angew. Chem., Int. Ed.* **2011**, *50*, 6415. (c) Avellini, T.; Li, H.; Coskun, A.; Barin, G.; Trabolsi, A.; Basuray, A. N.; Dey, S. K.; Credi, A.; Silvi, S.; Stoddart, J. F.; Venturi, M. *Angew. Chem., Int. Ed.* **2012**, *51*, 1611. (d) Wang, Z.-G.; Elbaz, J.; Willner, I. *Angew. Chem., Int. Ed.* **2012**, *51*, 4322. (e) Saha, M. L.; Smulders, M. M. J.; Jimenez, A.; Nitschke, J. R. *Angew. Chem., Int. Ed.* **2012**, *51*, 6681. (f) Pramanik, S.; Schmittel, M. *Chem. Commun.* **2012**, *48*, 9459. (g) Orentas, E.; Lista, M.; Lin, N. T.; Sakai, N.; Matile, S. *Nat. Chem.* **2012**, *4*, 746.

(10) For recent, detailed studies on host–guest binding dynamics, see: (a) Barrett, E. S.; Dale, T. J.; Rebek, J., Jr. *J. Am. Chem. Soc.* **2008**, *130*, 2344. (b) Tang, H.; Fuentealba, D.; Ko, Y. H.; Selvapalam, N.; Kim, K.; Bohne, C. J. *Am. Chem. Soc.* **2011**, *133*, 20623. (c) Rieth, S.; Badjic, J. D. *Chem.—Eur. J.* **2011**, *17*, 2562. (d) Baroncini, M.; Silvi, S.; Venturi, M.; Credi, A. *Angew. Chem., Int. Ed.* **2012**, *51*, 4223.

(11) (a) Arduini, A.; Calzavacca, F.; Pochini, A.; Secchi, A. *Chem.—Eur. J.* **2003**, *9*, 793. (b) Arduini, A.; Ciesa, F.; Fragassi, M.; Pochini, A.; Secchi, A. *Angew. Chem., Int. Ed.* **2005**, *44*, 278. (c) Arduini, A.; Bussolati, R.; Credi, A.; Faimani, G.; Garaudée, S.; Pochini, A.; Secchi, A.; Semeraro, M.; Silvi, S.; Venturi, M. *Chem.—Eur. J.* **2009**, *15*, 3230.

(12) For related studies, see: (a) Franchi, P.; Lucarini, M.; Pedulli, G. F.; Sciotto, D. *Angew. Chem., Int. Ed.* **2000**, *38*, 236. (b) Linnartz, P.; Schalley, C. A. *Supramol. Chem.* **2004**, *16*, 263. (c) Oshikiri, T.; Takashima, Y.; Yamaguchi, H.; Harada, A. *J. Am. Chem. Soc.* **2005**, *127*, 12186. (d) Wang, Q.-C.; Ma, X.; Qu, D.-H.; Tian, H. *Chem.—Eur. J.* **2006**, *12*, 1088. (e) Park, J. W. *J. Phys. Chem. B* **2006**, *110*, 24915. (f) Oshikiri, T.; Takashima, Y.; Yamaguchi, H.; Harada, A. *Chem.—Eur. J.* **2007**, *13*, 7091. (g) Park, J. W.; Song, H. J.; Cho, Y. J.; Park, K. *J. Phys. Chem. C* **2007**, *111*, 18605. (h) Franchi, P.; Casati, C.; Mezzina, E.; Lucarini, M. *Org. Biomol. Chem.* **2011**, *9*, 6396. (i) Casati, C.; Franchi, P.; Pievo, R.; Mezzina, E.; Lucarini, M. *J. Am. Chem. Soc.* **2012**, *134*, 19108. (k) Arduini, A.; Bussolati, R.; Credi, A.; Monaco, S.; Secchi, A.; Silvi, S.; Venturi, M. *Chem.—Eur. J.* **2012**, *18*, 16203.

(13) C₆D₆ was selected as the solvent for structural determinations as it allows a reliable assessment of the orientation of the axle threaded into **1**.¹¹ It is noteworthy that the uncomplexed axles are insoluble in this solvent.

(14) (a) Lee, Y.; Lee, C. *Bull. Korean Chem. Soc.* **1999**, *20*, 187. (b) Marotta, E.; Rastrelli, F.; Saielli, G. *J. Phys. Chem. B* **2008**, *112*, 16566.

(15) Credi, A.; Dumas, S.; Silvi, S.; Venturi, M.; Arduini, A.; Pochini, A.; Secchi, A. *J. Org. Chem.* **2004**, *69*, 5881.

(16) (a) Mukhopadhyay, P.; Zabalij, P. Y.; Isaacs, L. *J. Am. Chem. Soc.* **2006**, *128*, 14093. (b) Masson, E.; Lu, X.; Ling, X.; Patchell, D. L. *Org. Lett.* **2009**, *11*, 3798. (c) Jiang, W.; Schäfer, A.; Mohr, P. C.; Schalley, C. A. *J. Am. Chem. Soc.* **2010**, *132*, 2309.

(17) Oae, S.; Togo, H. *Bull. Chem. Soc. Jpn.* **1983**, *56*, 3813.

(18) Yoshida, Y.; Sakakura, Y.; Aso, N.; Okada, S.; Tanabe, Y. *Tetrahedron* **1999**, *55*, 2183.

(19) Kabalka, G. W.; Varma, M.; Varma, S. *J. Org. Chem.* **1986**, *51*, 2387.

(20) Sekera, C. V.; Marvel, C. S. *J. Am. Chem. Soc.* **1933**, *55*, 345.

(21) Boccia, A.; Lanzillotto, V.; Zanoni, R.; Pescatori, L.; Arduini, A.; Secchi, A. *Phys. Chem. Chem. Phys.* **2011**, *13*, 4444.

(22) Arduini, A.; Ferdani, R.; Pochini, A.; Secchi, A.; Ugozzoli, F. *Angew. Chem., Int. Ed.* **2000**, *39*, 3453.

(23) Binstead, R. A. *SPECFIT*; Spectrum Software Associates: Chapel Hill, NC, 1996.